MOLECULAR AND CELLULAR BIOLOGY, Sept. 2010, p. 4094–4107 Vol. 30, No. 17
0270-7306/10/$12.00 doi:10.1128/MCB.00246-10

Myristoylation and Membrane Binding Regulate c-Src Stability and Kinase Activity▽

Parag Patwardhan and Marilyn D. Resh*

Cell Biology Program, Memorial Sloan-Kettering Cancer Center, New York, New York 10065

Received 3 March 2010/Returned for modification 5 April 2010/Accepted 16 June 2010

Myristoylation is critical for membrane association of Src kinases, but a role for myristate in regulating other aspects of Src biology has not been explored. In the c-Abl tyrosine kinase, myristate binds within a hydrophobic pocket at the base of the kinase domain and latches the protein into an autoinhibitory conformation. A similar pocket has been predicted to exist in c-Src, raising the possibility that Src might also be regulated by myristoylation. Here we show that in contrast to the case for c-Abl, myristoylation exerts a positive effect on c-Src kinase activity. We also demonstrate that myristoylation and membrane binding regulate c-Src ubiquitination and degradation. Nonmyristoylated c-Src exhibited reduced kinase activity but had enhanced stability compared to myristoylated c-Src. We then mutated critical residues in the predicted myristate binding pocket of c-Src. Mutation of L360 and/or E486 had no effect on c-Src membrane binding or localization. However, constructs containing a T456A mutation were partially released from the membrane, suggesting that mutagenesis could induce c-Src to undergo an artificial myristoyl switch. All of the pocket mutants exhibited decreased kinase activity. We concluded that myristoylation and the pocket residues regulate c-Src, but in a manner very different from that for c-Abl.

Src family kinases (SFKs) are nonreceptor tyrosine kinases that act as key mediators of cellular signal transduction (12). The nine SFK members, Src, Yes, Fyn, Hck, Lck, Lyn, Blk, Fgr, and Yrk, play crucial roles in cellular proliferation, survival, migration, and growth factor and cytokine stimulation pathways (26, 39, 56). All SFKs share a similar domain arrangement, consisting of SH3, SH2, and kinase (SH1) domains as well as a unique domain and a membrane-targeting SH4 region at the N terminus (11). Crystal structures have shown that the catalytic activity of SFKs is tightly regulated by autoinhibition. The SH3 domain binds to a polyproline region in the linker between the SH2 and kinase domains, and the SH2 domain binds to a phosphotyrosine residue (Tyr527 in avian c-Src) near the C terminus. Kinase activation can be achieved by displacing one or all of the autoinhibitory interactions (52, 59, 60).

All SFKs are myristoylated at the N terminus (47). Myristoylation occurs cotranslationally and is catalyzed by the enzyme *N*-myristoyl transferase (NMT) (19). The 14-carbon saturated fatty acid myristate is covalently attached to the N-terminal glycine residue via an amide bond, making myristoylation an essentially irreversible modification (44, 48, 49). Myristoylation is necessary but not sufficient to anchor a protein to the membrane, and membrane binding of myristoylated proteins requires a second signal. For Src, the second signal is a polybasic cluster of amino acids that interacts with acidic phospholipids on the inner leaflet of the membrane bilayer (34, 35, 44, 46, 53). Nearly all other SFKs are instead modified by attachment of the 16-carbon saturated fatty acid palmitate to cysteine residues 3 and 5 or 6 at the N terminus (48). Myristoylation and palmitoylation together form a "dual signal" motif that targets SFKs to membranes.

Membrane binding is crucial for cellular functions mediated by Src and other SFKs. Nonmyristoylated forms of Src are cytoplasmic and cannot induce cellular transformation (14, 28, 29, 33). Membrane localization of c-Src has been shown to be important for dephosphorylation of Tyr527 and for mitotic activation of c-Src kinase activity (8), presumably because the phosphatase that acts on Tyr527 is membrane bound. Myristoylation has also been proposed to play a role in regulating nuclear transport of c-Src (17).

For some myristoylated proteins, the myristate moiety can exist in two different conformational states, either sequestered inside a hydrophobic pocket within the protein or exposed and available for membrane binding (44, 48). Binding to a ligand or another protein can cause a switch from one state to another, resulting in membrane association or dissociation. "Myristoyl switch" mechanisms have been identified in a variety of myristoylated proteins, including recoverin and HIV-1 Gag (4–6, 43, 45, 55). In the c-Abl tyrosine kinase, a "myristoyl phosphotyrosine" switch is operative. Myristate binds within a hydrophobic pocket at the base of the c-Abl kinase domain, docking the SH2 domain against the kinase domain in such a way that it prevents activation of the kinase by phosphotyrosine ligands (22, 36). A similar pocket is predicted to exist at the base of the c-Src kinase domain, raising the possibility that c-Src in the autoinhibited form might be capable of binding its own N-terminal myristate group in a manner similar to that of c-Abl (16). To date, only nonmyristoylated, N-terminally truncated forms of c-Src have been crystallized, and the position of the myristate within the full-length c-Src protein is not known. A recent study provided support for the existence of a potential myristate binding pocket within c-Src (16). Exogenous addition of myristate to the Tyr527-phosphorylated form of nonmyris-

* Corresponding author. Mailing address: Cell Biology Program, Memorial Sloan-Kettering Cancer Center, 1275 York Avenue, Box 143, New York, NY 10065. Phone: (212) 639-2514. Fax: (212) 717-3317. E-mail: m-resh@ski.mskcc.org.

▽ Published ahead of print on 28 June 2010.

toylated c-Src induced chemical shift changes in the nuclear magnetic resonance (NMR) spectra for both the protein and the fatty acid. However, the site of myristate binding was not determined. Thus, it is still not known how or if myristate regulates c-Src kinase activity and whether the predicted myristate binding pocket functions within c-Src in a manner similar to that of c-Abl.

In this study, we directly analyzed the role of myristoylation in regulating c-Src kinase activity and tested whether residues in the predicted myristate binding pocket contribute to myristate binding and/or c-Src activity. Here we show that myristoylation plays a positive role in regulating c-Src kinase activity. In contrast to c-Abl, nonmyristoylated c-Src exhibits reduced kinase activity both *in vitro* and in cells. We also made the surprising finding that the myristoylation status of c-Src determines its intracellular stability by regulating c-Src ubiquitination and degradation of the E3 ligase Cbl. Lastly, we analyzed the role of the predicted myristate binding pocket at the base of the c-Src kinase domain. Mutations in the pocket region resulted in decreased kinase activity and, with the exception of one mutation (Thr456Ala), had no effect on membrane binding of c-Src. We concluded that c-Src kinase activity is regulated by myristoylation, but in a different manner from that of c-Abl, and that a "myristoyl switch" is unlikely to be operative within c-Src.

MATERIALS AND METHODS

Reagents and antibodies. Rabbit polyclonal anti-c-Src (N-16), anti-caveolin-1 (N-20), anti-Cbl (C-15), and anti-Cas (C-20), mouse monoclonal anti-pTyr (PY99), anti-Lck (3A5), and anti-Lyn (44), and protein A/G plus agarose were purchased from Santa Cruz Biotechnology Inc. (Santa Cruz, CA). Polyclonal rabbit antiactin antibody, rabbit muscle enolase, and 2-hydroxymyristate (2-OHMyr) were purchased from Sigma (St. Louis, MO). Rabbit anti-phospho-c-Src (Y416) and anti-phospho-c-Src (Y527) antibodies were purchased from Cell Signaling Technology (Danvers, MA). Mouse monoclonal anti-Src antibody (clone GD11) was purchased from Millipore. Mouse monoclonal anti-Fyn and anti-Cbl antibodies were purchased from BD Transduction Laboratories (San Diego, CA). Mouse monoclonal antihemagglutinin (anti-HA; 12CA5) antibody was purchased from Roche. Tran^{35}S Cys/Met was purchased from MP Biomedicals (Solon, OH). [γ-^{32}P]ATP and Na^{125}I were purchased from Perkin Elmer (Waltham, MA).

Plasmid construction, cell culture, and transfection. Plasmids encoding monomeric c-SrcEYFP have been described previously (18). pCMV5 plasmids encoding G2A, 5N, Y527F/5N, Y527F/G2A, K295R, L360A, T456A, E486A, L360A/T456A, L360A/E486A, T456A/E486A, and L360A/T456A/E486A mutants of chicken c-Src were generated by site-directed mutagenesis, using a QuikChange mutagenesis kit (Stratagene). All constructs and mutations were confirmed by DNA sequencing. A plasmid encoding hemagglutinin (HA)-ubiquitin was a gift from Xuejun Jiang (Sloan Kettering Institute, NY). A plasmid encoding HA-Cbl was a gift from Dafna Bar-Sagi (New York University, NY). A baculoviral plasmid encoding wild-type (WT) Cas and SYF cells (Src/Yes/Fyn null) were gifts from Todd Miller (State University of New York at Stony Brook, NY). COS-1 and SYF cells were grown and maintained as described previously (18, 31). Cells were transfected using Lipofectamine 2000 (Invitrogen) according to the manufacturer's instructions. Plasmid DNA amounts of 2 to 5 μg were used for transfecting cells in 100-mm tissue culture dishes.

Western immunoblotting and immunoprecipitation. COS-1 cells were lysed in 1× RIPA buffer (50 mM Tris, pH 8.0, 150 mM NaCl, 1% NP-40, 0.5% deoxycholate, 0.1% SDS, 1 mM EDTA, 1 mM Na_3VO_4) containing 10 mg/ml aprotinin, 10 mg/ml leupeptin, and 250 mg/ml 4-(2-aminoethyl) benzene sulfonyl fluoride (AEBSF). SYF cells were lysed in EB++ buffer as described previously (31). Lysates were cleared by centrifugation at 100,000 × *g* at 4°C for 10 min. Protein concentrations were measured using a DC protein assay kit (Bio-Rad), and equal amounts of protein were loaded into the gel. Immunoprecipitation was carried out by incubating equal amounts of lysates with antibody at 4°C overnight. Samples were centrifuged, washed three times with cold lysis buffer, resuspended in 2× SDS-PAGE sample buffer, and boiled. For the detection of ubiquitinated Src, RIPA lysates or equal volumes of the soluble fraction (S100) and the pellet fraction (P100) were mixed with 1% SDS, vortexed, and boiled. Lysates were then diluted 5-fold with TBS (50 mM Tris, pH 7.5, 120 mM NaCl) and centrifuged at 100,000 × *g* for 30 min. Cleared lysates were used for overnight immunoprecipitation, using a homemade rabbit polyclonal anti-Src or anti-Fyn antibody (produced in the Resh lab). Total cell lysates or immunoprecipitated samples were loaded into 8% or 10% SDS-PAGE gels and transferred to polyvinylidene difluoride (PVDF) membranes, and immunoblotting was performed with the appropriate antibodies. Proteins were detected using secondary antibodies conjugated to horseradish peroxidase and Pierce enhanced chemiluminescence (Thermo Scientific, IL). Western blots were scanned and quantified using a Bio-Rad GS800 scanning densitometer and QuantityOne software.

2-Hydroxymyristate treatment and metabolic labeling. Transfected COS-1 cells were treated with 2-hydroxymyristate as described previously (57). Briefly, cells were preincubated with 1 mM 2-hydroxymyristate in Dulbecco's modified Eagle's medium (DMEM) containing 1% defatted bovine serum albumin (BSA) for 2 h at 37°C. DMEM containing 5% fetal bovine serum (FBS) was then added, followed by overnight incubation with 500 μM 2-hydroxymyristate. ^{35}S pulse-chase and synthesis analyses were performed at 22 to 24 h posttransfection. Transfected COS-1 cells were starved for 1 h in DMEM without cysteine and methionine [DMEM (−Cys/−Met)] supplemented with 2% dialyzed FBS. For pulse-chase experiments, cells were pulsed for 15 to 20 min with DMEM (−Cys/−Met) containing 50 μCi/ml Tran^{35}S label at 37°C and then chased for various times with DMEM containing 10% FBS and an excess of unlabeled cysteine and methionine. For the ^{35}S-labeled protein synthesis assay, cells were starved as described above and then labeled with 50 μCi/ml Tran^{35}S label at 37°C for various times. At each time point, cells were lysed in RIPA buffer, and lysates were immunoprecipitated and subjected to phosphorimaging as described previously (18). Synthesis and radiolabeling of 13-[^{125}I]iodotridecanoic acid have been described previously (41), and radioiodinated fatty acid labeling was carried out as described previously (3). For metabolic labeling assays, phosphorimaging screens were analyzed on a FLA-7000 phosphorimager (Fuji) and quantitated using ImageGauge software.

***In vitro* kinase assay.** COS-1 cells were lysed in lysis buffer (10 mM Tris, pH 7.2, 100 mM NaCl, 1 mM EDTA, 1% NP-40, 0.5% deoxycholate) containing protease inhibitors. Lysates were cleared by centrifugation at 100,000 × *g* at 4°C for 10 min. Protein concentration was measured using a DC protein assay kit (Bio-Rad), and immunoprecipitation was performed by incubating equal amounts of lysates with a rabbit polyclonal anti-Src antibody (produced in the Resh lab) and protein A/G plus agarose overnight at 4°C. Samples were centrifuged and then washed three times with cold lysis buffer and twice with kinase assay buffer (20 mM HEPES, pH 7.4, 5 mM $MgCl_2$, 5 mM $MnCl_2$) containing 1 mM Na_3VO_4. Protein A/G-agarose beads were resuspended in kinase assay buffer and incubated at 30°C with 5 μg acid-denatured rabbit muscle enolase or 0.5 to 1 μM Ni-nitrilotriacetic acid (Ni-NTA)-purified wild-type Cas (40), 100 μM unlabeled ATP, and 5 to 10 μCi [γ-^{32}P]ATP per reaction mixture. At various time points, the reaction was stopped by adding 2× SDS-PAGE sample buffer and boiling the samples. Samples were resolved in 10% SDS-PAGE gels, stained with Coomassie blue to ensure equal loading of enolase and Cas, dried, and exposed to X-ray film (Kodak) or a phosphorimager screen for 12 to 24 h. Phosphorimaging screens were analyzed on a FLA-7000 phosphorimager (Fuji) and quantitated using ImageGauge software.

Cell fractionation. Cell fractionation was carried out as described previously, with minor modifications (58). Briefly, COS-1 cells cotransfected with plasmids encoding c-Src and NMT were analyzed at 44 to 46 h posttransfection. Cells were washed with cold STE buffer (50 mM Tris, pH 7.2, 150 mM NaCl, 1 mM EDTA), resuspended in hypotonic buffer (10 mM Tris-HCl, pH 7.2, 0.2 mM $MgCl_2$) supplemented with protease inhibitors, and incubated on ice for 10 min, followed by homogenization with 30 strokes in a 1.5-ml Dounce homogenizer with a tight pestle or by sonication with two pulses of 30 s each. The homogenate was adjusted to 250 mM sucrose and 1 mM EDTA and centrifuged for 30 to 45 min at 100,000 × *g* (50,000 rpm in a TLA 100.2 rotor) or 200,000 × *g* (100,000 rpm) in an Optima TL ultracentrifuge (Beckman Instruments, CA). The pellet (P100), containing total cellular membranes, was resuspended in 1× RIPA buffer supplemented with protease inhibitors, and the soluble fraction (S100) was supplemented with a 0.2 volume of 5× concentrated RIPA buffer. Samples were incubated for 15 to 30 min on ice and clarified by centrifugation for 15 min at 100,000 × *g*. Equal volumes of the S100 and P100 fractions were loaded into 10% SDS-PAGE gels, and immunoblotting was performed with the appropriate antibodies.

Indirect immunofluorescence assay. COS-1 cells were split at 24 h posttransfection onto 22- by 22-mm coverslips, placed in 6-well dishes, and analyzed for c-Src expression at 48 h posttransfection as described previously (18), using

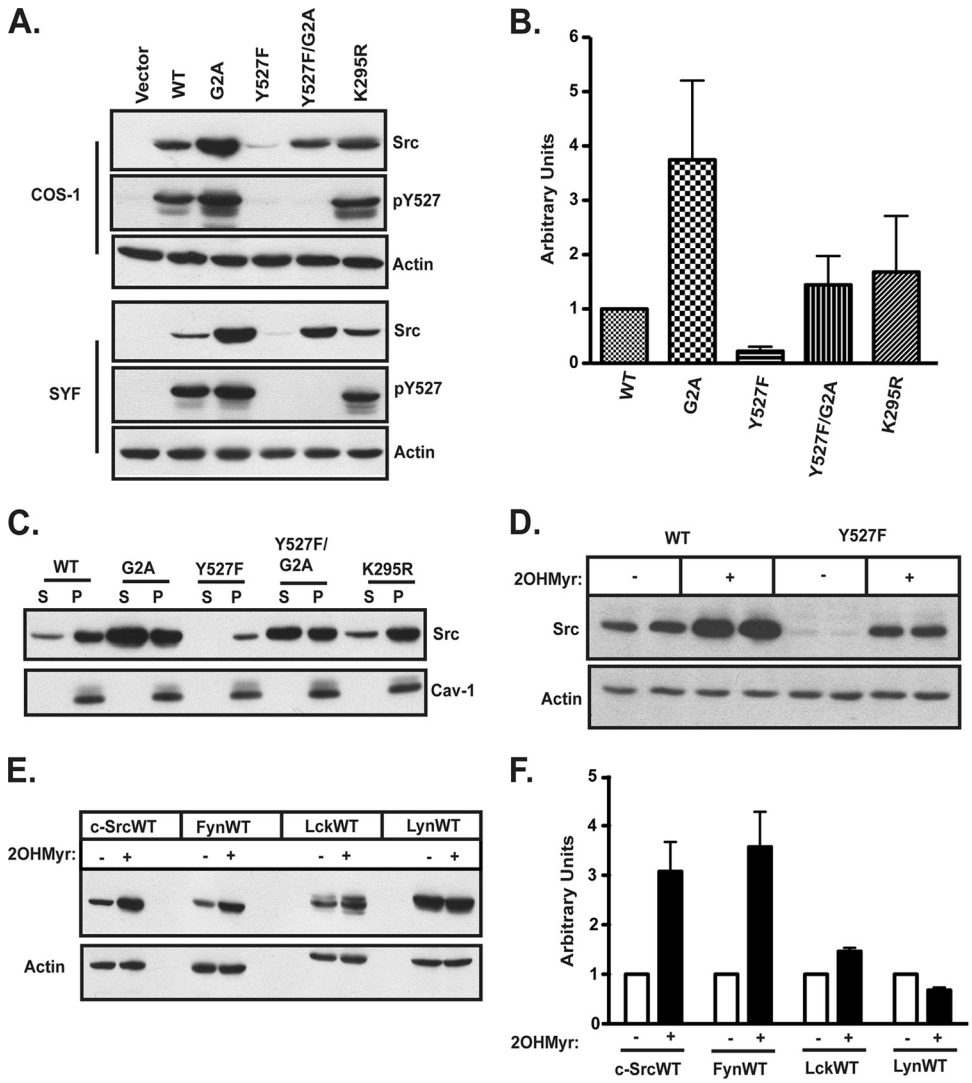

FIG. 1. Steady-state levels of WT and mutant Src family kinases. (A) COS-1 or SYF cells were transfected with the indicated c-Src constructs, and at 44 to 46 h posttransfection, cell lysates were analyzed by Western blotting, using anti-c-Src, anti-phospho-c-SrcY527, and antiactin antibodies. (B) Quantification of c-Src expression levels in COS-1 cells, as determined by Western blotting, normalized to c-SrcWT expression (set to 1). Combined data from three independent experiments are shown. Error bars represent standard deviations. (C) Subcellular distribution of c-SrcWT and mutants. COS-1 cells cotransfected with the indicated c-Src constructs and NMT were subjected to cell fractionation. Equal volumes of the soluble (S) and membrane pellet (P) fractions were analyzed by Western blotting, using anti-c-Src and anti-caveolin-1 antibodies. (D and E) Steady-state levels of Src family kinases after 2-hydroxymyristate treatment. COS-1 cells transfected with the indicated constructs were treated overnight with 2-hydroxymyristate or dimethyl sulfoxide (DMSO), and cell lysates were analyzed by SDS-PAGE and Western blotting with appropriate antibodies. (F) Quantification of the experiment in panel E. For each kinase, the steady-state level after 2-hydroxymyristate treatment is shown relative to the DMSO control level, which was set to 1. The averages for three independent experiments are shown. Error bars represent standard deviations.

anti-c-Src (N-16) antibody. Coverslips were mounted onto microscope slides by use of Prolong Gold antifade reagent (Molecular Probes). Images were obtained on a Zeiss LSM510 confocal microscope equipped with an Axiovert 100 M inverted microscope, using a ×63, 1.2-numerical-aperture water immersion lens.

RESULTS

Nonmyristoylated c-Src exhibits higher levels of expression than myristoylated c-Src. To determine the role of myristoylation in modulating Src structure and function, COS-1 cells and SYF (Src/Yes/Fyn null) fibroblasts (31) were transfected with plasmids encoding WT and various mutant forms of c-Src. Steady-state expression levels were strikingly different for the different c-Src constructs. Compared to levels of WT c-Src (c-SrcWT), the expression level of c-SrcY527F, an activated mutant in which the negative-regulatory Tyr527 residue is mutated to phenylalanine, was 4- to 5-fold lower (Fig. 1A and B), consistent with findings of previous reports (23). Decreased expression of c-SrcY527F was likely due to its increased kinase activity, as levels of the catalytically inactive c-SrcK295R construct were equivalent to those of c-SrcWT. In contrast, the levels of nonmyristoylated (G2A) forms of c-Src and c-SrcY527F were 4-fold and 6-fold higher than those of

c-SrcWT and c-SrcY527F, respectively (Fig. 1A and B). Similar results were obtained for the nonmyristoylated mutant of another Src family kinase member, Fyn (see Fig. 5A) (3). These findings suggest that nonmyristoylated forms of c-Src might have more stability than their myristoylated counterparts.

The extent of membrane association was determined for WT and mutant c-Src proteins (Fig. 1C). Nearly 80 to 90% of WT, Y527F, and K295R c-Src proteins were localized to the membrane fraction, indicating that the activation state of c-Src does not influence the overall extent of membrane binding. In contrast, G2A c-Src and Y527F/G2A c-Src exhibited a predominantly soluble distribution.

Steady-state levels of Src family kinases are increased by treatment with 2-hydroxymyristate. Treatment with 2-OHMyr, a potent inhibitor of NMT (38), can be used as an alternative method to block myristoylation in cells. When COS-1 cells were transfected with c-SrcWT or c-SrcY527F and then treated with 2-OHMyr (57), levels of both c-SrcWT and c-SrcY527F (Fig. 1D) were elevated. An increase in the level of another Src family kinase, Fyn, was also observed in 2-OHMyr-treated cells, whereas little to no change was observed for Lck and Lyn (Fig. 1E and F). These findings establish that myristoylation regulates the expression levels of at least two Src family kinases.

Nonmyristoylated c-Src is degraded more slowly than wild-type c-Src. We next sought to determine whether the increased steady-state level of nonmyristoylated c-Src was due to alterations in protein synthesis or degradation. Pulse-chase analysis was carried out using COS-1 cells transfected with c-SrcWT or c-SrcG2A. The half-life of c-SrcG2A (~11.5 h) was longer than that of c-SrcWT (~7 h) (Fig. 2A), whereas the rates of synthesis for the two proteins were equivalent (Fig. 2B). These findings suggest that slower degradation, but not increased synthesis, might account for the observed increase in c-SrcG2A protein levels.

Active but not nonmyristoylated forms of c-Src are targeted for ubiquitination. Earlier studies reported that activated forms of Src kinase serve as targets for the ubiquitin-mediated degradation pathway (21, 23). We wished to determine whether the myristoylation state of c-Src affects ubiquitination. SYF fibroblasts as well as COS-1 cells were cotransfected with or without HA-tagged ubiquitin and either empty vector or cDNA encoding c-SrcWT, c-SrcG2A, c-SrcY527F, or c-SrcY527F/G2A. c-Src was immunoprecipitated from the lysates and probed with anti-HA and anti-Src antibodies. Ubiquitinated forms of c-SrcY527F were readily detectable in the anti-HA immunoprecipitates, as a smear of high-molecular-weight bands, in both COS-1 (Fig. 3A) and SYF (data not shown) cells. Ubiquitinated forms of c-SrcWT were also observed, consistent with the fact that c-SrcWT maintains basal levels of kinase activity. In contrast, few to no high-molecular-weight bands were observed for the nonmyristoylated mutants c-SrcG2A and c-SrcY527F/G2A, despite the fact that the latter construct retains the activating mutation at Tyr527 (Fig. 3A). These data suggest that the myristoylation status influences ubiquitin-mediated degradation of Src kinases.

Nonmyristoylated c-Src is not subject to Cbl-mediated downregulation and is defective in targeting Cbl for degradation. Previous reports have shown that c-Cbl can act as an E3 ubiquitin ligase for downregulation of Src kinases (7, 20). In

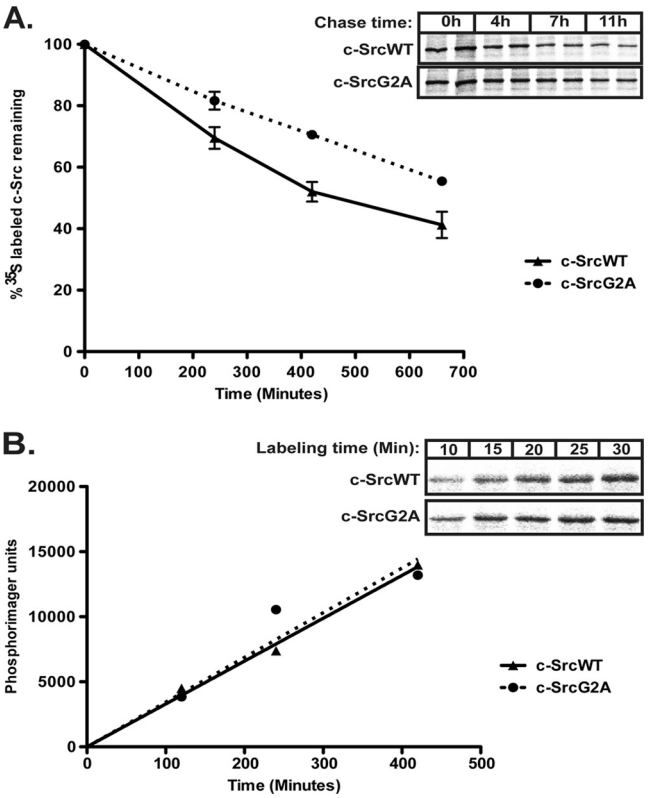

FIG. 2. Synthesis and degradation rates of WT and nonmyristoylated c-Src. (A) COS-1 cells were transfected with the indicated c-Src constructs. At 22 to 24 h posttransfection, cells were pulse labeled for 15 to 20 min in DMEM containing Tran^{35}S-labeled cysteine-methionine and chased in nonradioactive medium for the indicated times. At each time point, c-Src was immunoprecipitated from the cell lysates, and the amount of labeled c-Src was quantified and plotted relative to the amount of c-Src at time zero (100%). Average data for 2 independent experiments performed in duplicate are shown. (B) COS-1 cells transfected with the indicated c-Src constructs were pulse labeled with medium containing Tran^{35}S-labeled cysteine-methionine for the indicated times, c-Src was immunoprecipitated, and the amount of labeled c-Src was quantified and plotted as a function of time. The inset shows autoradiographs for time points between 10 and 30 min. Representative data from experiments performed at least two times in duplicate are shown.

order to examine the interplay between c-Src and Cbl, COS-1 cells were cotransfected with or without HA-tagged Cbl and cDNAs encoding either WT or mutant forms of c-Src. With coexpression with Cbl, decreases were detected in c-SrcWT and c-SrcY527F levels, but no change in either c-SrcG2A or c-SrcK295R levels was apparent (Fig. 3B, top panels). The effects of c-Src expression on Cbl were much more dramatic. Levels of Cbl were drastically reduced when c-SrcWT was coexpressed and were reduced even further when the activated mutant c-SrcY527F was coexpressed. In contrast, coexpression of either c-SrcG2A or c-SrcK295R with Cbl had no effect on Cbl levels (Fig. 3B, middle panels), suggesting that myristoylation and Src kinase activity are required for Cbl degradation.

Pulse-chase analysis was carried out to analyze Cbl stability. The half-life of Cbl was ~5.5 h in the presence of c-SrcWT (Fig. 3C) but was appreciably longer, ~8 to 8.5 h, when Cbl was expressed either alone or in the presence of c-SrcG2A.

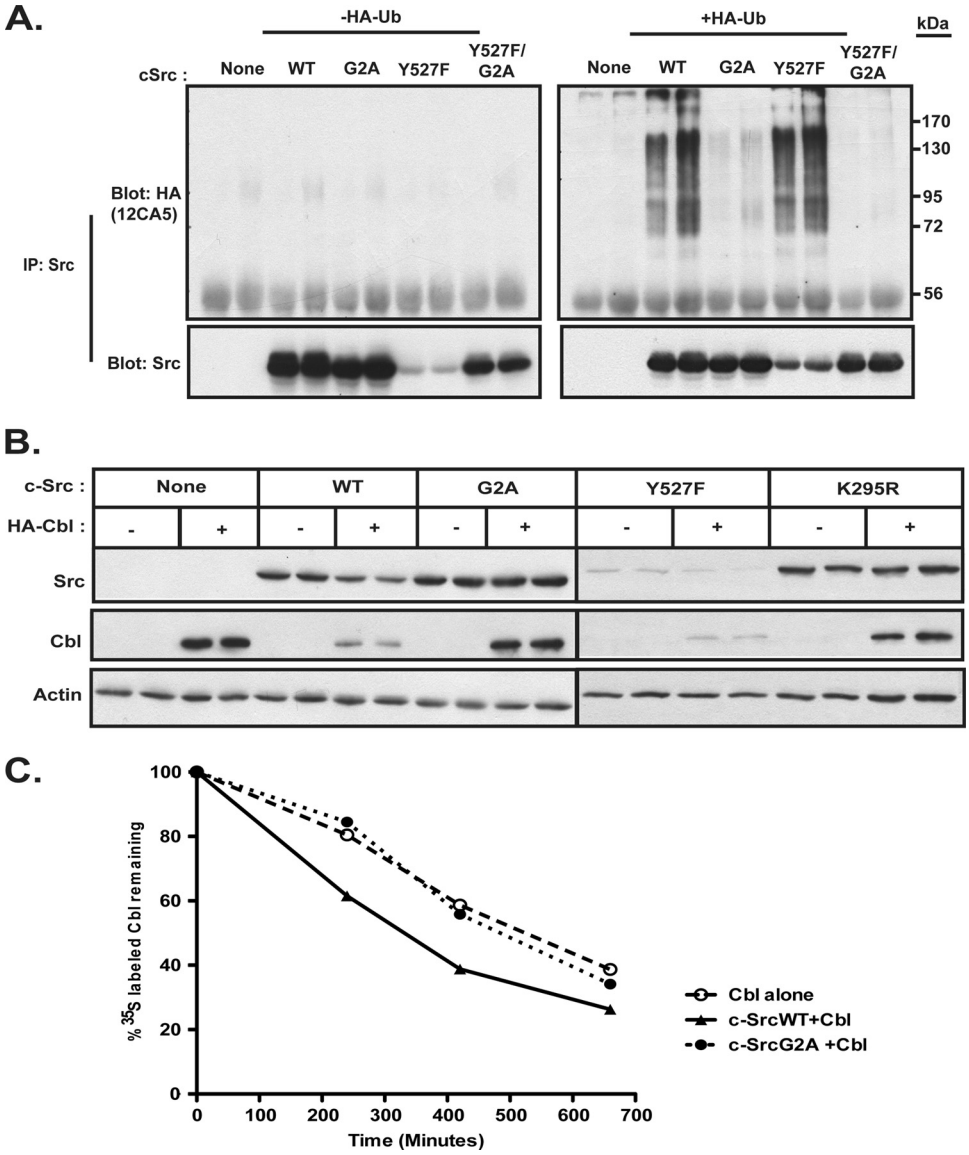

FIG. 3. Ubiquitination, steady-state levels, and stability of myristoylated and nonmyristoylated c-Src. (A) COS-1 cells were transfected with the indicated c-Src constructs, either alone or with HA-tagged ubiquitin. At 48 h posttransfection, cells were treated with 25 μM MG132 at 37°C for 2 h, lysed, and treated with 1% SDS. c-Src was immunoprecipitated, and samples were analyzed by Western blotting with anti-Src (GD11) and anti-HA (12CA5) antibodies. (B) COS-1 cells were cotransfected with the indicated c-Src constructs and either empty vector or a vector encoding HA-tagged Cbl. At 48 h posttransfection, cell lysates were analyzed by Western blotting using the indicated antibodies. (C) COS-1 cells transfected with HA-Cbl alone or with the indicated c-Src constructs were pulse labeled as described in Materials and Methods. Cbl was immunoprecipitated from cell lysates. The amount of radiolabeled Cbl was quantified by phosphorimaging and plotted relative to the amount at time zero (100%). Representative data for two independent experiments performed in duplicate are shown.

These findings indicate that nonmyristoylated c-Src is neither downregulated by Cbl nor capable of targeting Cbl for degradation.

Membrane association is necessary for ubiquitination of SFKs. We next set out to determine whether the effect of myristoylation on c-Src stability and ubiquitination was due to a direct effect of the myristate moiety on c-Src or the result of the ability of myristate to promote targeting of c-Src to the membrane. To distinguish between these two models, we analyzed a c-Src mutant that maintains the N-terminal myristoylation site but lacks the second, polybasic membrane targeting signal (34, 35, 44, 46, 53). This construct, c-Src5N, has 5 of the 6 basic residues in the N-terminal region of c-Src (Lys5, Lys9, and Arg14, -15, and -16) mutated to Asn; Lys7 is known to be critical for myristoylation of Src (30) and was not mutated.

WT and mutant forms of c-Src were expressed by transient transfection in COS-1 cells. Compared to c-SrcWT, c-Src5N showed increased levels of expression, similar to those of the G2A mutant (Fig. 4A). Radiolabeling of the cells with ^{125}I-IC13, a radioiodinated myristate analog (41), revealed that c-Src5N was myristoylated, but only 30 to 40% as efficiently as c-SrcWT (Fig. 4B). It has been shown previously (57) that

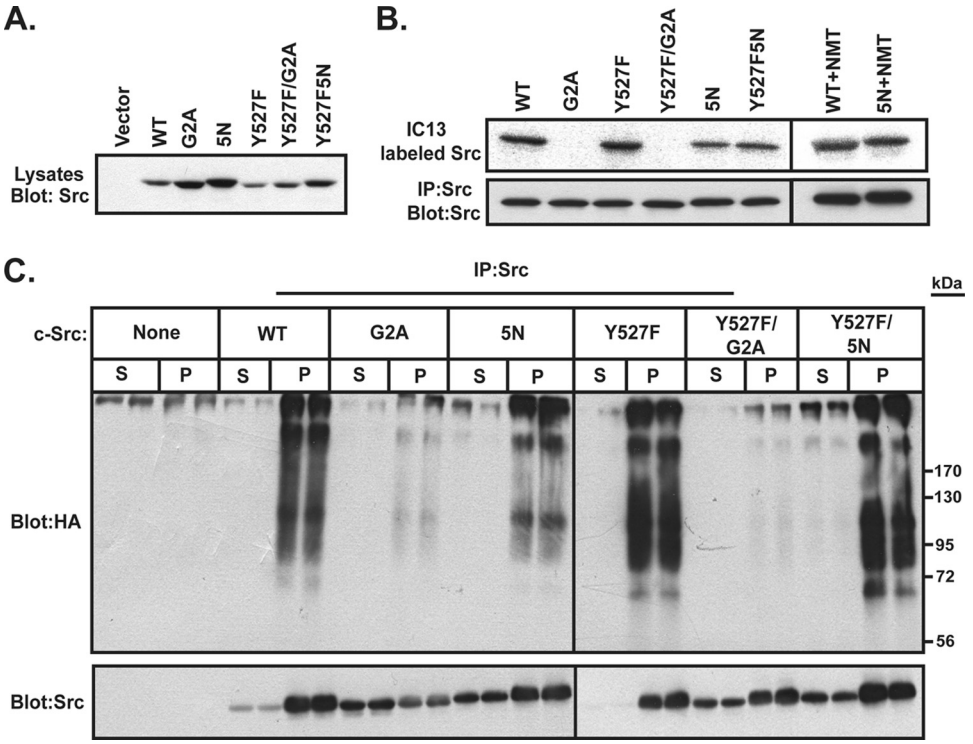

FIG. 4. Analysis of polybasic cluster mutants of c-Src. (A) COS-1 cells were transfected with the indicated c-Src constructs. At 24 h posttransfection, lysates were analyzed by Western blotting using anti-SrcGD11 antibody. A representative blot from two independent experiments is shown. (B) COS-1 cells transfected with the indicated c-Src constructs, with or without NMT, were labeled with the myristate analog 13-[^{125}I]iodotridecanoic acid for 4 h at 37°C. c-Src was immunoprecipitated, and radiolabel incorporation was analyzed by SDS-PAGE and autoradiography. (C) COS-1 cells were cotransfected with the indicated c-Src constructs, NMT, and HA-tagged ubiquitin. At approximately 24 h posttransfection, cells were treated with 25 μM MG132 for 2 h at 37°C and then subjected to cell fractionation. Equal volumes of each fraction were treated with 1% SDS, c-Src was immunoprecipitated, and samples were analyzed by Western blotting, using anti-Src (GD11) and anti-HA (12CA5) antibodies.

mutating Lys at positions 7 and 9 in Fyn results in a defect in myristoylation. This defect can be rescued by coexpression of NMT (57). With coexpression with NMT, the defect in myristoylation of c-Src5N was rescued, as c-Src5N was myristoylated ~94% as efficiently as c-SrcWT (Fig. 4B). The effects of the 5N mutation on membrane association and polyubiquitination of c-Src were then assessed. COS-1 cells were cotransfected with WT or mutant forms of c-Src, HA-ubiquitin, and NMT. The cells were subjected to subcellular fractionation, and each fraction was immunoprecipitated with anti-Src antibody and probed with Src and HA antibodies. The 5N mutant versions of WT and Y527F c-Src displayed significantly more c-Src protein in the soluble fraction than their counterparts with native N termini (Fig. 4C). However, ubiquitinated forms of Src were detected only in the membrane fractions for WT, Y527F, 5N, and Y527F/5N c-Src (Fig. 4C). Ubiquitinated forms of nonmyristoylated (G2A) mutants of c-Src were not observed (Fig. 4C), confirming the results depicted in Fig. 3. Despite the presence of myristoylated c-Src5N in the soluble fraction, no ubiquitination ladder was evident in this fraction. These results suggest that membrane association, rather than myristoylation status, is the primary driving force for directing c-Src ubiquitination.

In order to test whether membrane binding can reverse a myristoylation defect, we artificially targeted a nonmyristoylated SFK to the membrane. The membrane targeting sequence from K-Ras was attached to the C terminus of Fyn (57), and the behavior of FynKRas was compared to that of WT and mutant forms of Fyn. Nonmyristoylated Fyn (G2A) partitioned mostly in the soluble fraction (70%) and showed increased levels of expression compared to WT Fyn (Fig. 5A and B), a finding similar to that observed for c-SrcG2A (Fig. 1A). WT Fyn containing the K-Ras membrane targeting sequence exhibited reduced levels of expression compared to WT Fyn (Fig. 5A), suggesting that tighter membrane association because of an additional membrane targeting signal results in decreased protein stability. Attachment of the K-Ras tail to G2AFyn redirected nearly all the G2AFynKRas to the membrane and resulted in a 3.7-fold decrease in protein expression compared to that for G2AFyn (Fig. 5A and B). This decrease was reversed (Fig. 5A) when the critical Cys residue in the membrane targeting signal of K-Ras was mutated (C552S). These findings indicate that targeting nonmyristoylated Fyn to the membrane results in decreased stability.

To test the dependence of ubiquitination on myristoylation and membrane association, COS-1 cells were cotransfected with WT or mutant forms of Fyn and HA-ubiquitin. Ubiquitinated forms of Fyn were observed for WT Fyn and WT-FynKRas (Fig. 5C). Similar to c-SrcG2A, nonmyristoylated Fyn (G2A) did not show the presence of a ubiquitin ladder

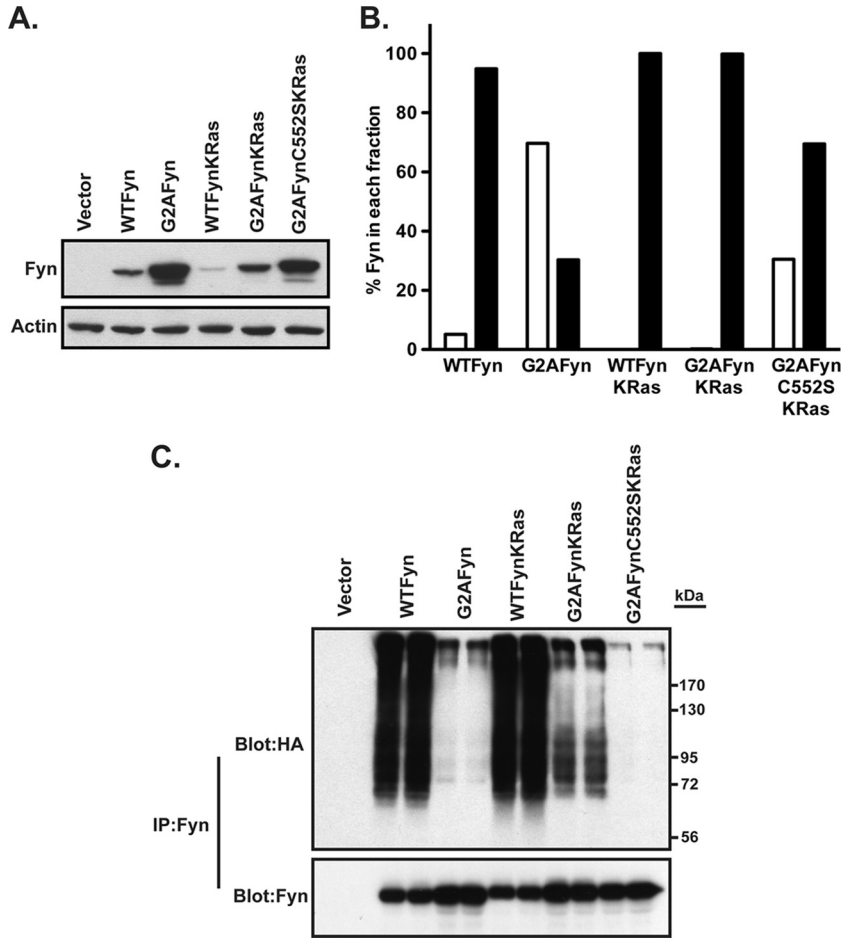

FIG. 5. Analysis of Fyn mutants containing a K-Ras membrane targeting signal. (A and B) COS-1 cells were transfected with the indicated Fyn constructs. At 48 h posttransfection, lysates were analyzed by Western blotting with anti-Fyn and antiactin antibodies (A), or cells were subjected to cell fractionation (B). Equal volumes of each fraction were analyzed by Western blotting, using anti-Fyn antibody, and were quantified using densitometry. Open bars = S100; closed bars = P100. (C) COS-1 cells were cotransfected with the indicated Fyn constructs and HA-tagged ubiquitin. At 22 to 24 h posttransfection, cells were treated with 25 μM MG132 for 2 h at 37°C and lysed in RIPA buffer, lysates were treated with 1% SDS, Fyn was immunoprecipitated, and samples were analyzed by Western blotting with anti-Fyn and anti-HA (12CA5) antibodies.

(Fig. 5C). Notably, high-molecular-weight ubiquitinated forms were detected for G2AFynKRas but not for the C552S version of this construct. These results strongly suggest that membrane targeting can restore polyubiquitination of Fyn even in the absence of an N-terminal myristate.

Nonmyristoylated c-Src has reduced kinase activity. We next analyzed the effect of myristoylation on c-Src kinase activity. We first performed *in vitro* kinase assays to quantify the ability of c-SrcWT and c-SrcG2A to phosphorylate exogenous substrates. COS-1 cells were transfected with c-SrcWT or c-SrcG2A. We made two adjustments in an attempt to equalize expression of the two proteins: smaller amounts of cDNA were used for c-SrcG2A transfectants, and cells were harvested at 22 to 24 h (rather than 48 h) posttransfection. Under these conditions, similar levels of Src expression were obtained for c-SrcWT and c-SrcG2A (Fig. 6A and B). c-Src was immunoprecipitated from the cell lysates and then subjected to an *in vitro* kinase assay, using [γ-^{32}P]ATP and either enolase or p130Cas, a physiologic Src substrate, as exogenous substrates. As depicted in Fig. 6A and B, c-SrcG2A was clearly defective in phosphorylating either substrate, a finding that strongly supports the conclusion that the myristoylation state of the protein plays a crucial role in kinase activity.

In order to determine whether nonmyristoylated c-Src could phosphorylate Cas in cells, SYF fibroblasts (which have high levels of endogenous p130Cas) were transfected with WT or mutant forms of c-Src. Cas was immunoprecipitated from the lysates, and the immunoprecipitates were probed with antiphosphotyrosine antibody. Cells transfected with c-SrcY527F displayed the highest levels of tyrosine-phosphorylated Cas (Fig. 6C, middle panel), despite having the lowest levels of Src present in the lysate (Fig. 6C, top panel). However, when c-SrcY527F/G2A was expressed, the level of tyrosine-phosphorylated Cas was ~3-fold lower. c-SrcWT was able to phosphorylate Cas, whereas cells expressing c-SrcG2A exhibited reduced Cas phosphorylation (Fig. 6C, middle panel). These data clearly demonstrate that myristoylation plays a positive role in the ability of c-Src to phosphorylate its substrates.

To determine whether membrane association played a role in regulating kinase activity, we analyzed the distribution of

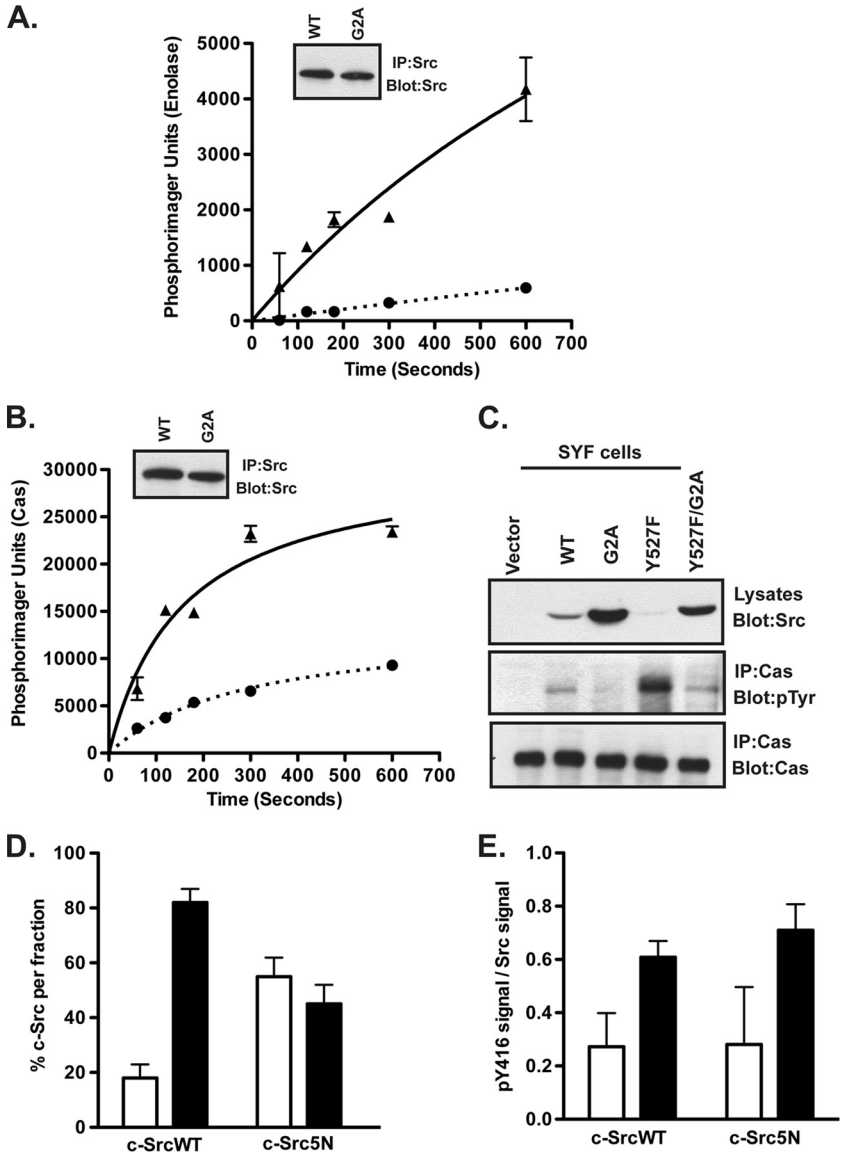

FIG. 6. Nonmyristoylated c-Src exhibits reduced kinase activity. (A and B) COS-1 cells were transfected with WT or G2A c-Src constructs. At 24 h posttransfection, c-Src was immunoprecipitated and subjected to an *in vitro* kinase assay using enolase or purified p130Cas. The amounts of phosphorylated enolase (A) and Cas (B) were quantified by phosphorimaging and plotted as a function of time. Triangles = WT; circles = G2A mutant. Average data for two independent experiments are shown. Error bars indicate standard deviations. Insets show that equal amounts of c-SrcWT and c-SrcG2A were immunoprecipitated. (C) SYF cells transfected with WT or mutant c-Src constructs were lysed at 24 h posttransfection, and endogenous Cas was immunoprecipitated. Lysates and immunoprecipitated samples were analyzed by Western blotting with the indicated antibodies. (D and E) 3T3 cells stably expressing c-SrcWT and c-Src5N were subjected to cell fractionation. Equal volumes of the S100 and P100 fractions were analyzed by Western blotting, using anti-Src (GD11) (D) or anti-phospho-c-Src (Y416) (E) antibody, and were quantified using densitometry. Combined data for two independent experiments are shown. Open bars = S100; closed bars = P100.

activated (pY416) c-Src in membrane and soluble fractions by using 3T3 cells stably expressing c-SrcWT or c-Src5N. Approximately 60% of c-Src5N partitioned in the soluble fraction, compared to 20% for c-SrcWT (Fig. 6D). On a per-unit basis, activated c-Src kinase (pY416) was found primarily in the membrane fraction (Fig. 6E), suggesting that membrane-bound c-Src is preferentially catalytically active.

Residues lining the predicted myristate binding pocket in c-Src affect kinase activity. Crystal structures of c-Abl, a related tyrosine kinase, have shown that the N-terminal myristoyl group binds to a pocket at the base of the kinase domain and plays a role in autoinhibiting the kinase (22, 36). Based on the sequence similarity between the kinase domains of c-Abl and Src, another study predicted that there could be a potential "myristate binding pocket" in Src kinase as well (16). However, several residues lining the predicted binding pocket are bulkier in c-Src than in c-Abl and are therefore likely to prevent the myristoyl group from interacting with the kinase domain (36). We chose to mutate three critical residues, Leu360, Thr456, and Glu486, in an attempt to make this region more accessible

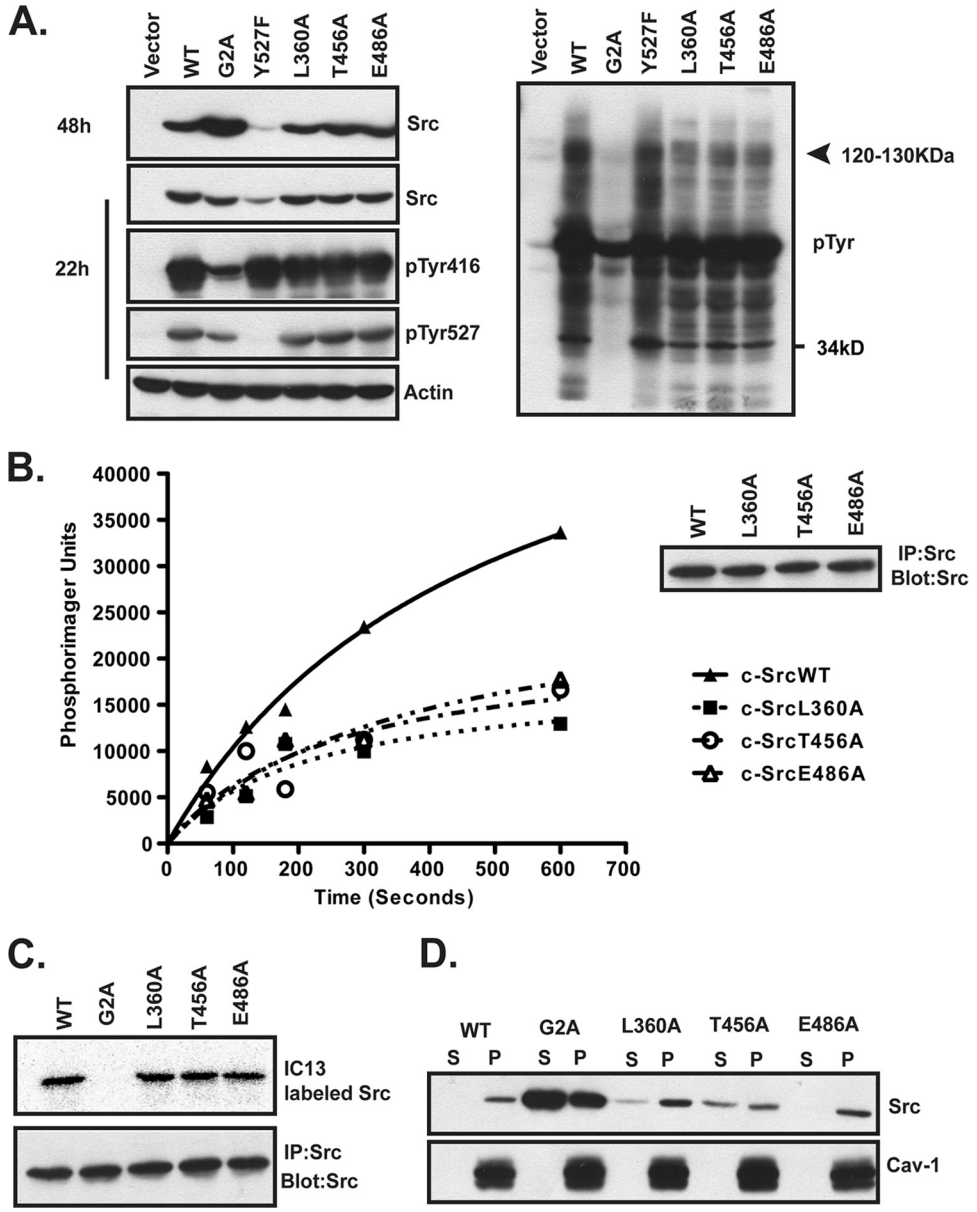

FIG. 7. Analysis of single-site "pocket" mutants of c-Src. (A) COS-1 cells transfected with WT and mutant c-Src constructs were lysed at 22 or 48 h posttransfection, and lysates were analyzed by Western blotting with the indicated antibodies. (B) COS-1 cells transfected with WT or mutant c-Src were lysed at 24 h posttransfection. c-Src was immunoprecipitated and used in an *in vitro* kinase assay with purified Cas. Representative data from two independent experiments performed in duplicate are shown. The inset shows that equal amounts of WT and mutant Src were immunoprecipitated. (C) COS-1 cells transfected with the indicated c-Src constructs were labeled with the myristate analog 13-[^{125}I]iodotridecanoic acid for 4 h at 37°C. c-Src was immunoprecipitated, and radiolabel incorporation was analyzed by SDS-PAGE and autoradiography. (D) Lysates from COS-1 cells cotransfected with NMT and WT or mutant c-Src were subjected to cell fractionation and analyzed as described in the legend to Fig. 1C.

for myristate binding. If any of these "pocket" mutations result in opening up the pocket, and if myristate then becomes sequestered in this pocket, then the mutant protein should behave in a manner similar to that of nonmyristoylated c-Src.

COS-1 cells were transfected with constructs encoding WT or mutant c-Src and then harvested at 48 h posttransfection, and Src expression, kinase activity, myristoylation, and membrane binding were analyzed. c-SrcWT and all three pocket mutants showed similar levels of expression (Fig. 7A, left side, panel 1). As observed earlier, c-SrcY527F was expressed at lower levels, whereas c-SrcG2A was expressed at much higher levels than those of c-SrcWT. By adjusting the amount of DNA transfected and harvesting cells at 22 h posttransfection, equivalent levels of expression were achieved for c-SrcWT, c-SrcG2A, and the three pocket mutants (Fig. 7A, left side, panel 2). c-SrcWT and all three pocket mutants exhibited similar levels of phosphorylation at Tyr416 and Tyr527 (Fig. 7A, left side, panels 3 and 4). Although c-SrcG2A displayed similar

levels of phosphorylation at Tyr527 to those for c-SrcWT, it had a significantly reduced signal for phosphorylation at Tyr416 on a per-unit basis, indicating that autophosphorylation levels were lower (Fig. 7A, left side, panels 3 and 4). Total phosphotyrosine (pTyr) content was also reduced in lysates from cells expressing c-SrcG2A compared to those from cells expressing c-SrcWT and the other mutants (Fig. 7A, right panel). In addition, lysates from cells expressing each of the three pocket mutants exhibited lower pTyr levels than did those from cells expressing c-SrcWT and c-SrcY527F, especially in the range of 120 to 130 kDa (Fig. 7A, right panel).

Since Cas is a known endogenous substrate of Src that migrates in the 120- to 130-kDa range, we carried out an *in vitro* kinase assay to assess the ability of the pocket mutants to phosphorylate purified Cas. c-SrcWT displayed robust phosphorylation of Cas, but all three pocket mutants were defective in phosphorylating Cas (Fig. 7B). These data suggest that at least one of the bands observed in the pTyr blot in the range of 120 to 130 kDa represents Cas (Fig. 7A). Thus, the three residues in the predicted myristate binding pocket do not play a physiologic role in the accessibility of the C-terminal Tyr527 residue to Csk but are important for maintaining optimal kinase activity and exogenous substrate phosphorylation.

If mutation of any of the pocket residues resulted in opening up the pocket for myristate binding and sequestration, we would expect to observe a shift in the membrane binding properties of the mutant protein. All three pocket mutants were myristoylated to the same extent as c-SrcWT (Fig. 7C). The L360A and E486A c-Src mutants exhibited the same extent of membrane association (>90%) as that of c-SrcWT (Fig. 7D). However, introduction of the T456A mutation resulted in a partial shift of the mutant c-Src into the soluble fraction (~35% in the soluble fraction and ~65% in the membrane fraction). We therefore tested whether double or triple mutants might exhibit further alterations in membrane binding and/or kinase activity.

COS-1 cells were transfected with constructs encoding c-SrcWT or mutants containing the L360A, T456A, and E486A mutations in double or triple combinations. Similar to the single-site mutants, all four multisite mutants were expressed at levels essentially equivalent to those of c-SrcWT at both 22 h and 48 h posttransfection (Fig. 8A, panels 1 and 3). All of the mutants exhibited similar levels of phosphorylation at Tyr527 (Fig. 8A, panels 2 and 4) and of myristoylation (Fig. 8B) to those for c-SrcWT. c-SrcWT as well as the L360A/E486A mutant partitioned >90% in the membrane fraction. However, constructs containing double and triple mutations of T456 combined with the other two residues exhibited increased distribution in the soluble fraction. The T456A/E486A mutant was equally distributed in the soluble and membrane fractions, and double or triple mutants containing L360A and T456A partitioned ~75 to 80% in the soluble fraction (Fig. 8C).

The subcellular localization of the c-Src pocket mutants was determined using indirect immunofluorescence. c-SrcWT showed a characteristic perinuclear distribution and plasma membrane association, while c-SrcG2A exhibited a scattered distribution throughout the cytoplasm (Fig. 8D) (18). The double (T456A/E486A) and triple (L360A/T456A/E486A) mutants also exhibited perinuclear distribution and membrane association similar to those of c-SrcWT (Fig. 8D), but increased cytoplasmic staining for both mutants was readily detected, consistent with the fractionation studies. Lastly, *in vitro* kinase assays using purified Cas revealed that none of the 3 mutants tested could phosphorylate Cas efficiently (Fig. 8E). These findings indicate that myristoylation and the pocket residues are important for full activity of c-Src but function in a manner very different from that for c-Abl.

DISCUSSION

Myristoylation regulates c-Src stability. Tight control of the levels of c-Src protein and tyrosine kinase activity is critical for regulation of the growth of normal and cancer cells. Here we reveal a hitherto unappreciated role of the N-terminal myristate moiety in regulating steady-state levels and kinase activity of c-Src. In a direct comparison, expression levels of nonmyristoylated (G2A) mutant forms of c-Src were 4- to 6-fold higher than those of their myristoylated counterparts. The increased expression could not be attributed to introduction of a mutated N-terminal residue (Ala), because treatment of cells expressing c-SrcWT with 2-hydroxymyristate resulted in the same phenotype as that for c-SrcG2A. Comparison of the rates of protein synthesis and degradation revealed that c-SrcG2A exhibits a longer half-life than that of c-SrcWT. These findings argue that regulation of steady-state levels of c-Src occurs at the level of protein stability.

Previous studies have established that activated forms of c-Src are targeted for ubiquitination and degradation. We have confirmed and extended these findings by showing that nonmyristoylated c-Src does not exhibit the characteristic polyubiquitin ladder that is clearly evident for Y527F and WT c-Src proteins. Thus, it is likely that a lack of or reduced ubiquitination allows nonmyristoylated c-Src to resist proteasome-mediated degradation. The mechanistic basis for the differences observed between WT and nonmyristoylated c-Src could be due to a requirement for the myristate moiety *per se* in driving ubiquitination of the protein or a result of the ability of myristate to promote targeting of c-Src to the membrane. Our data obtained using a polybasic mutant of c-Src and mutants of Fyn that are artificially targeted to the membrane (Fig. 4 and 5) support the second possibility. However, note that the ubiquitination signal on G2AFynKRas was not as strong as that on WTFyn or WTFynKRas. It is likely that membrane attachment via a C-terminal tail rather than the physiologic N-terminal signal affects protein conformation and possibly restricts accessibility to the ubiquitination machinery.

Multiple lines of evidence point to the ubiquitin E3 ligase Cbl as a key regulator of ubiquitination and degradation of the SFKs Src, Fyn, Lyn, and Hck (7, 9, 20, 24, 27, 42, 61). Interdependent ubiquitination and degradation of Src and Cbl have also been demonstrated (61). When c-Src and Cbl were coexpressed, we observed a decrease in c-SrcWT levels (Fig. 3B) that was not detected for G2A or K295R c-Src. A significant amount of c-SrcWT remained even when Cbl was coexpressed, suggesting that Cbl is not the only E3 ligase that regulates c-Src stability. This is consistent with findings from other reports that identified two additional E3 ubiquitin ligases, cullin-5 and E6AP (32, 37), responsible for modulating SFK ubiquitination and degradation. However, c-Src expression induced a striking decrease in the levels of Cbl, and this effect was not observed

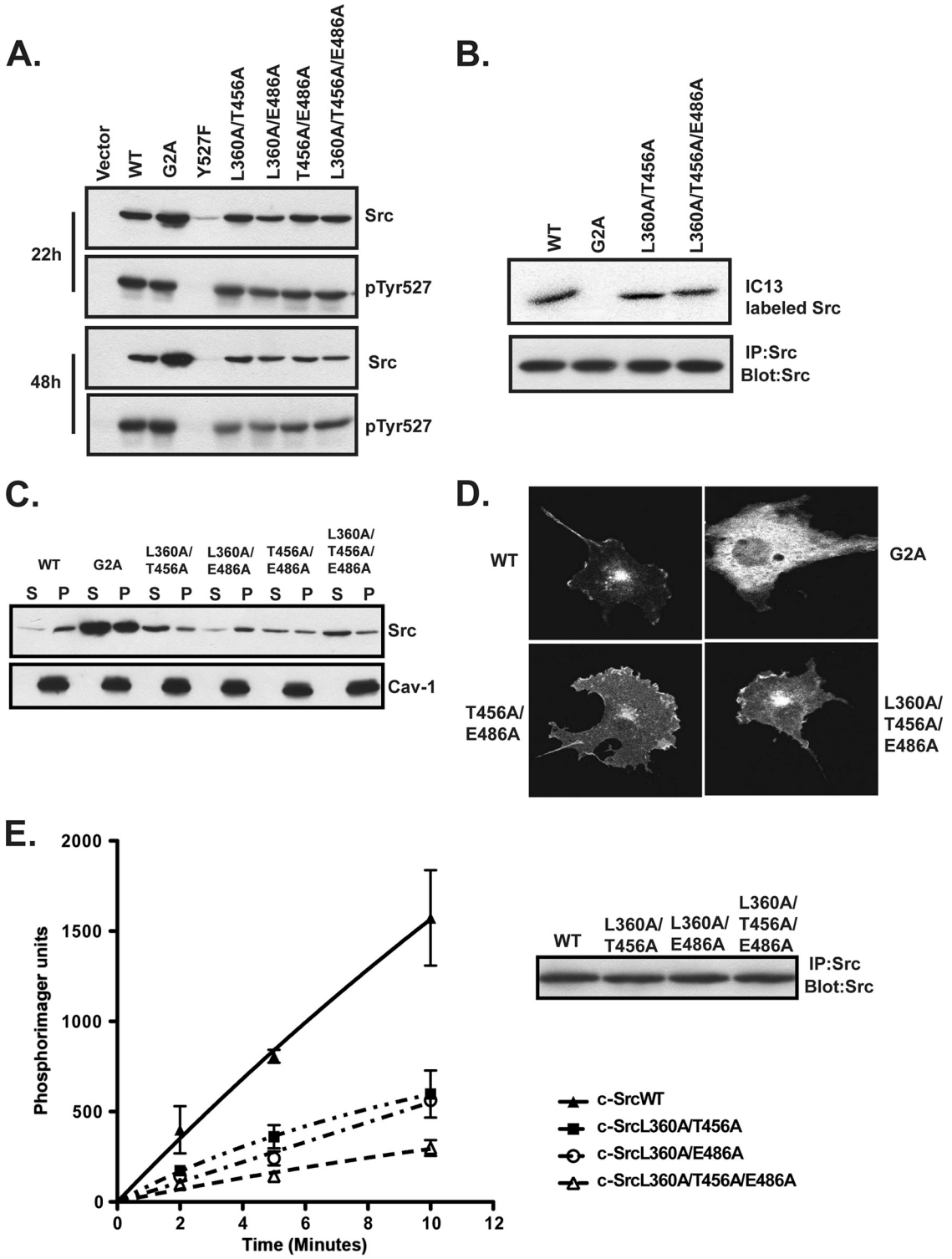

FIG. 8. Analysis of multisite "pocket" mutants of c-Src. (A) COS-1 cells transfected with WT and mutant c-Src constructs were lysed at 22 or 48 h posttransfection, and lysates were analyzed by Western blotting with the indicated antibodies. (B) COS-1 cells transfected with WT or mutant c-Src constructs were labeled with 13-[^{125}I]iodotridecanoic acid, and radiolabel incorporation into c-Src was analyzed as described in the legend to Fig. 7C. (C) Lysates from COS-1 cells cotransfected with NMT and WT or mutant c-Src were subjected to cell fractionation and analyzed as described in the legend to Fig. 1C. (D) COS-1 cells transfected with WT or mutant c-Src were analyzed at 48 h posttransfection for c-Src expression, using indirect immunofluorescence. (E) COS-1 cells transfected with WT or mutant c-Src were lysed at 24 h posttransfection. c-Src was immunoprecipitated and used in an *in vitro* kinase assay with purified Cas. Combined data from two independent experiments are shown. Error bars indicate standard deviations. The inset shows that equal amounts of WT and mutant Src were immunoprecipitated.

with c-SrcG2A (Fig. 3). Moreover, association with and phosphorylation of Cbl by c-SrcG2A were reduced compared to those with c-SrcWT (data not shown). A subpopulation of Cbl proteins has been reported to be membrane bound, and membrane binding enhances the ability of Cbl to ubiquitinate membrane-bound targets (24, 54). Our data suggest that the reduced accessibility of nonmyristoylated c-Src to Cbl and other E3 ubiquitin ligases limits the extent of c-SrcG2A ubiquitination and degradation and contributes to the increased expression levels compared to those of c-SrcWT.

The pocket that binds myristate in c-Abl does not sequester myristate in c-Src. Biochemical and structural studies of c-Abl indicate that myristate binds within a deep hydrophobic pocket at the base of the c-Abl tyrosine kinase domain (22, 36). Cowan-Jacob et al. (16) solved the crystal structure of a partially active, unphosphorylated form of c-Src and showed that the C-terminal tail binds to a "pocket" equivalent to the c-Abl myristate binding pocket (36). In the autoinhibited form of c-Src, the C-terminal tail is phosphorylated and would be extruded from the pocket. Based on the sequence similarity between c-Src and c-Abl, it was suggested that myristate could now bind in the c-Src pocket (16). NMR spectroscopic data (16) suggested that myristate can bind to the phosphorylated (Tyr527) form of c-Src, but the exact site of myristate binding was not determined. Using the PYMOL molecular graphics program, we modeled the structures of inactive, phosphorylated c-Src (59) and c-Abl (36) within the predicted regions of similarity. The predicted "pocket" in c-Src exists but is much narrower than the myristate binding pocket in Abl due to steric hindrance by the c-Src bulky side chains (data not shown). Our modeling also indicated that the side chains of the residues lining the wall protrude into the predicted "pocket" and therefore would interfere with any potential myristate binding. Cowan-Jacob et al. suggested that minor conformational changes might allow this "pocket" to accommodate myristate within the inactive, Tyr527-phosphorylated form of c-Src (16). However, a study by Nagar et al. notes that three of the critical residues that line the myristate binding pocket within c-Abl are replaced by bulkier residues in c-Src (36), and they predicted that these bulkier residues would block binding of myristate to this site in c-Src. Here we verified the latter prediction by showing that WT, activated, and kinase-inactive forms of c-Src are all almost entirely (80 to 90%) membrane bound (Fig. 1), consistent with myristate being in an "exposed" conformation. Extensive studies by our laboratory and others have established that myristate is a major contributor to membrane association of Src (13, 44, 46, 47, 50, 53). If myristate were partially or totally sequestered within c-Src, we would have expected to detect a significant amount of soluble, myristoylated c-Src. Further support for our claim that myristate does not bind in the pocket region of c-Src comes from studies of GNF-2, an allosteric inhibitor of Bcr-Abl. GNF-2 binds within the myristate binding pocket of Abl and inhibits Bcr-Abl kinase (62), but this compound has no effect on the kinase activity of c-Src or other SFKs (2). We concluded that the pocket that binds myristate in c-Abl does not perform an analogous function for c-Src, making it unlikely that c-Src undergoes a myristoyl switch.

We tested whether mutagenesis of the three critical pocket residues in c-Src could artificially open the pocket to accommodate binding of a myristate moiety. Mutation of two of the three residues, L360 and E486, either alone or in combination, had no effect on c-Src membrane binding or subcellular localization (Fig. 7 and 8). However, mutation of T456, either alone or in combination with L360 and/or E486, resulted in increased amounts of c-Src in the soluble, cytosolic fraction. One explanation for these findings is that upon mutagenesis of the critical pocket residues in c-Src to mimic those of c-Abl, c-Src undergoes an artificially induced myristoyl switch and is released from the membrane. It is important, however, that the T456A mutants still retained membrane localization and expression levels characteristic of c-SrcWT and thus did not fully mimic the behavior of c-SrcG2A. Thus, at this point, generation of an artificial myristoyl switch remains a speculation. Alternatively, myristate may become partially sequestered in the pocket mutants, but not in the pocket region. It is possible that the pocket mutations expose a different region of c-Src that accommodates myristate binding. Another possibility is that the pocket residues might be involved in positioning of the kinase and/or SH2 domains, both of which have been shown to play a role in promoting membrane association of c-Src (51). In the absence of a three-dimensional structure for myristoylated c-Src, further extensive mutagenesis would be required to distinguish among these possibilities.

Myristoylation regulates c-Src tyrosine kinase activity. Myristoylation negatively regulates the tyrosine kinase activity of c-Abl. Here we show that the opposite is true for c-Src. Assays performed *in vitro* and in cells revealed that nonmyristoylated forms of c-Src exhibited reduced levels of tyrosine kinase activity (Fig. 6). This finding is in agreement with another report that noted lower kinase activity in unsynchronized cells for c-SrcG2A than that for c-SrcWT (8). Mutation of the myristoylation site in Lck, another SFK, has been shown to result in reduced kinase activity (1). Treatment of cells with the methionine aminopeptidase inhibitor bengamide A blocks removal of the initiator methionine residue and thereby prevents N-myristoylation. c-Src synthesized in bengamide A-treated cells exhibits decreased kinase activity, both *in vitro* and *in vivo* (25). We concluded that myristate plays a positive role in regulating c-Src kinase activity.

Regulation of c-Abl tyrosine kinase activity is due to interaction of its N-terminal myristate with residues in the myristate binding pocket. We explored the contributions of three critical pocket residues to the kinase activity of c-Src. Our data clearly demonstrate that mutation of each of these three residues to Ala, in single, double, or triple combinations, resulted in a reduction of c-Src kinase activity. It is unlikely that the decreased kinase activities observed for all of the pocket mutants can be attributed to insertion of myristate into the pocket, because membrane binding and subcellular localization of the L360 and E486 mutants, either alone or in combination, were not altered. No apparent changes in the extent of Tyr527 phosphorylation were detected, suggesting that accessibility of the C-terminal tail to Csk was not affected by the mutations. The defect in kinase activity observed for the c-Src pocket mutants could potentially be due to changes in the conformation of the kinase domain and/or positioning of other domains rather than to the position of myristate within the protein.

How does myristate enhance the tyrosine kinase activity of c-Src? One possibility is that by mediating insertion into a lipid

bilayer in the cell or into a detergent micelle *in vitro*, myristate serves to orient c-Src molecules in a conformation optimal for kinase activity. Autophosphorylation of c-Src, which is necessary for activation, is believed to occur via an intermolecular reaction (10, 15). Alignment of myristoylated c-Src molecules along a lipophilic surface may facilitate close or oriented packing of c-Src polypeptides and thereby promote phosphorylation in *trans*. Our finding that c-SrcG2A exhibits decreased levels of autophosphorylation at Tyr416 is consistent with this hypothesis.

ACKNOWLEDGMENTS

We thank Raisa Louft-Nisenbaum for expert technical assistance and Kai Xu and Dimitar Nikolov for help with structural modeling.

This work was supported by Public Health Service grant GM57966 from the National Institute of General Medical Sciences and by postdoctoral fellowship PDF0504316 from the Susan G. Komen Foundation.

REFERENCES

1. **Abraham, N., and A. Veillette.** 1990. Activation of p56lck through mutation of a regulatory carboxy-terminal tyrosine residue requires intact sites of autophosphorylation and myristylation. Mol. Cell. Biol. **10:**5197–5206.
2. **Adrian, F. J., Q. Ding, T. Sim, A. Velentza, C. Sloan, Y. Liu, G. Zhang, W. Hur, S. Ding, P. Manley, J. Mestan, D. Fabbro, and N. S. Gray.** 2006. Allosteric inhibitors of Bcr-abl-dependent cell proliferation. Nat. Chem. Biol. **2:**95–102.
3. **Alland, L., S. M. Peseckis, R. E. Atherton, L. Berthiaume, and M. D. Resh.** 1994. Dual myristylation and palmitylation of Src family member p59fyn affects subcellular localization. J. Biol. Chem. **269:**16701–16705.
4. **Ames, J. B., T. Porumb, T. Tanaka, M. Ikura, and L. Stryer.** 1995. Amino-terminal myristoylation induces cooperative calcium binding to recoverin. J. Biol. Chem. **270:**4526–4533.
5. **Ames, J. B., T. Tanaka, M. Ikura, and L. Stryer.** 1995. Nuclear magnetic resonance evidence for Ca(2+)-induced extrusion of the myristoyl group of recoverin. J. Biol. Chem. **270:**30909–30913.
6. **Ames, J. B., T. Tanaka, L. Stryer, and M. Ikura.** 1996. Portrait of a myristoyl switch protein. Curr. Opin. Struct. Biol. **6:**432–438.
7. **Andoniou, C. E., N. L. Lill, C. B. Thien, M. L. Lupher, Jr., S. Ota, D. D. Bowtell, R. M. Scaife, W. Y. Langdon, and H. Band.** 2000. The Cbl proto-oncogene product negatively regulates the Src-family tyrosine kinase Fyn by enhancing its degradation. Mol. Cell. Biol. **20:**851–867.
8. **Bagrodia, S., S. J. Taylor, and D. Shalloway.** 1993. Myristylation is required for Tyr-527 dephosphorylation and activation of pp60c-src in mitosis. Mol. Cell. Biol. **13:**1464–1470.
9. **Bao, J., G. Gur, and Y. Yarden.** 2003. Src promotes destruction of c-Cbl: implications for oncogenic synergy between Src and growth factor receptors. Proc. Natl. Acad. Sci. U. S. A. **100:**2438–2443.
10. **Barker, S. C., D. B. Kassel, D. Weigl, X. Huang, M. A. Luther, and W. B. Knight.** 1995. Characterization of pp60c-src tyrosine kinase activities using a continuous assay: autoactivation of the enzyme is an intermolecular autophosphorylation process. Biochemistry **34:**14843–14851.
11. **Boggon, T. J., and M. J. Eck.** 2004. Structure and regulation of Src family kinases. Oncogene **23:**7918–7927.
12. **Brown, M. T., and J. A. Cooper.** 1996. Regulation, substrates and functions of src. Biochim. Biophys. Acta **1287:**121–149.
13. **Buser, C. A., C. T. Sigal, M. D. Resh, and S. McLaughlin.** 1994. Membrane binding of myristylated peptides corresponding to the NH2 terminus of Src. Biochemistry **33:**13093–13101.
14. **Buss, J. E., M. P. Kamps, K. Gould, and B. M. Sefton.** 1986. The absence of myristic acid decreases membrane binding of p60src but does not affect tyrosine protein kinase activity. J. Virol. **58:**468–474.
15. **Cooper, J. A., and A. MacAuley.** 1988. Potential positive and negative autoregulation of p60c-src by intermolecular autophosphorylation. Proc. Natl. Acad. Sci. U. S. A. **85:**4232–4236.
16. **Cowan-Jacob, S. W., G. Fendrich, P. W. Manley, W. Jahnke, D. Fabbro, J. Liebetanz, and T. Meyer.** 2005. The crystal structure of a c-Src complex in an active conformation suggests possible steps in c-Src activation. Structure **13:**861–871.
17. **David-Pfeuty, T., S. Bagrodia, and D. Shalloway.** 1993. Differential localization patterns of myristoylated and nonmyristoylated c-Src proteins in interphase and mitotic c-Src overexpresser cells. J. Cell Sci. **105:**613–628.
18. **Donepudi, M., and M. D. Resh.** 2008. c-Src trafficking and co-localization with the EGF receptor promotes EGF ligand-independent EGF receptor activation and signaling. Cell. Signal. **20:**1359–1367.
19. **Farazi, T. A., G. Waksman, and J. I. Gordon.** 2001. The biology and enzymology of protein N-myristoylation. J. Biol. Chem. **276:**39501–39504.
20. **Ghosh, A. K., A. L. Reddi, N. L. Rao, L. Duan, V. Band, and H. Band.** 2004. Biochemical basis for the requirement of kinase activity for Cbl-dependent ubiquitinylation and degradation of a target tyrosine kinase. J. Biol. Chem. **279:**36132–36141.
21. **Hakak, Y., and G. S. Martin.** 1999. Ubiquitin-dependent degradation of active Src. Curr. Biol. **9:**1039–1042.
22. **Hantschel, O., B. Nagar, S. Guettler, J. Kretzschmar, K. Dorey, J. Kuriyan, and G. Superti-Furga.** 2003. A myristoyl/phosphotyrosine switch regulates c-Abl. Cell **112:**845–857.
23. **Harris, K. F., I. Shoji, E. M. Cooper, S. Kumar, H. Oda, and P. M. Howley.** 1999. Ubiquitin-mediated degradation of active Src tyrosine kinase. Proc. Natl. Acad. Sci. U. S. A. **96:**13738–13743.
24. **Howlett, C. J., and S. M. Robbins.** 2002. Membrane-anchored Cbl suppresses Hck protein-tyrosine kinase mediated cellular transformation. Oncogene **21:**1707–1716.
25. **Hu, X., Y. Dang, K. Tenney, P. Crews, C. W. Tsai, K. M. Sixt, P. A. Cole, and J. O. Liu.** 2007. Regulation of c-Src nonreceptor tyrosine kinase activity by bengamide A through inhibition of methionine aminopeptidases. Chem. Biol. **14:**764–774.
26. **Ingley, E.** 2008. Src family kinases: regulation of their activities, levels and identification of new pathways. Biochim. Biophys. Acta **1784:**56–65.
27. **Kaabeche, K., J. Lemonnier, S. Le Mee, J. Caverzasio, and P. J. Marie.** 2004. Cbl-mediated degradation of Lyn and Fyn induced by constitutive fibroblast growth factor receptor-2 activation supports osteoblast differentiation. J. Biol. Chem. **279:**36259–36267.
28. **Kamps, M. P., J. E. Buss, and B. M. Sefton.** 1985. Mutation of NH2-terminal glycine of p60src prevents both myristoylation and morphological transformation. Proc. Natl. Acad. Sci. U. S. A. **82:**4625–4628.
29. **Kamps, M. P., J. E. Buss, and B. M. Sefton.** 1986. Rous sarcoma virus transforming protein lacking myristic acid phosphorylates known polypeptide substrates without inducing transformation. Cell **45:**105–112.
30. **Kaplan, J. M., G. Mardon, J. M. Bishop, and H. E. Varmus.** 1988. The first seven amino acids encoded by the v-src oncogene act as a myristylation signal: lysine 7 is a critical determinant. Mol. Cell. Biol. **8:**2435–2441.
31. **Klinghoffer, R. A., C. Sachsenmaier, J. A. Cooper, and P. Soriano.** 1999. Src family kinases are required for integrin but not PDGFR signal transduction. EMBO J. **18:**2459–2471.
32. **Laszlo, G. S., and J. A. Cooper.** 2009. Restriction of Src activity by cullin-5. Curr. Biol. **19:**157–162.
33. **Linder, M. E., and J. G. Burr.** 1988. Nonmyristoylated p60v-src fails to phosphorylate proteins of 115–120 kDa in chicken embryo fibroblasts. Proc. Natl. Acad. Sci. U. S. A. **85:**2608–2612.
34. **McLaughlin, S., and A. Aderem.** 1995. The myristoyl-electrostatic switch: a modulator of reversible protein-membrane interactions. Trends Biochem. Sci. **20:**272–276.
35. **Murray, D., L. Hermida-Matsumoto, C. A. Buser, J. Tsang, C. T. Sigal, N. Ben-Tal, B. Honig, M. D. Resh, and S. McLaughlin.** 1998. Electrostatics and the membrane association of Src: theory and experiment. Biochemistry **37:**2145–2159.
36. **Nagar, B., O. Hantschel, M. A. Young, K. Scheffzek, D. Veach, W. Bornmann, B. Clarkson, G. Superti-Furga, and J. Kuriyan.** 2003. Structural basis for the autoinhibition of c-Abl tyrosine kinase. Cell **112:**859–871.
37. **Oda, H., S. Kumar, and P. M. Howley.** 1999. Regulation of the Src family tyrosine kinase Blk through E6AP-mediated ubiquitination. Proc. Natl. Acad. Sci. U. S. A. **96:**9557–9562.
38. **Paige, L. A., G. Q. Zheng, S. A. DeFrees, J. M. Cassady, and R. L. Geahlen.** 1990. Metabolic activation of 2-substituted derivatives of myristic acid to form potent inhibitors of myristoyl CoA:protein N-myristoyltransferase. Biochemistry **29:**10566–10573.
39. **Parsons, S. J., and J. T. Parsons.** 2004. Src family kinases, key regulators of signal transduction. Oncogene **23:**7906–7909.
40. **Patwardhan, P., Y. Shen, G. S. Goldberg, and W. T. Miller.** 2006. Individual Cas phosphorylation sites are dispensable for processive phosphorylation by Src and anchorage-independent cell growth. J. Biol. Chem. **281:**20689–20697.
41. **Peseckis, S. M., I. Deichaite, and M. D. Resh.** 1993. Iodinated fatty acids as probes for myristate processing and function. Incorporation into pp60v-src. J. Biol. Chem. **268:**5107–5114.
42. **Rao, N., S. Miyake, A. L. Reddi, P. Douillard, A. K. Ghosh, I. L. Dodge, P. Zhou, N. D. Fernandes, and H. Band.** 2002. Negative regulation of Lck by Cbl ubiquitin ligase. Proc. Natl. Acad. Sci. U. S. A. **99:**3794–3799.
43. **Resh, M. D.** 2004. A myristoyl switch regulates membrane binding of HIV-1 Gag. Proc. Natl. Acad. Sci. U. S. A. **101:**417–418.
44. **Resh, M. D.** 1999. Fatty acylation of proteins: new insights into membrane targeting of myristoylated and palmitoylated proteins. Biochim. Biophys. Acta **1451:**1–16.
45. **Resh, M. D.** 2005. Intracellular trafficking of HIV-1 Gag: how Gag interacts with cell membranes and makes viral particles. AIDS Rev. **7:**84–91.
46. **Resh, M. D.** 2004. Membrane targeting of lipid modified signal transduction proteins. Subcell. Biochem. **37:**217–232.
47. **Resh, M. D.** 1994. Myristylation and palmitylation of Src family members: the fats of the matter. Cell **76:**411–413.

48. **Resh, M. D.** 2006. Palmitoylation of ligands, receptors, and intracellular signaling molecules. Sci. STKE **2006:**re14.
49. **Resh, M. D.** 1996. Regulation of cellular signalling by fatty acid acylation and prenylation of signal transduction proteins. Cell. Signal. **8:**403–412.
50. **Resh, M. D.** 2006. Trafficking and signaling by fatty-acylated and prenylated proteins. Nat. Chem. Biol. **2:**584–590.
51. **Shvartsman, D. E., J. C. Donaldson, B. Diaz, O. Gutman, G. S. Martin, and Y. I. Henis.** 2007. Src kinase activity and SH2 domain regulate the dynamics of Src association with lipid and protein targets. J. Cell Biol. **178:**675–686.
52. **Sicheri, F., I. Moarefi, and J. Kuriyan.** 1997. Crystal structure of the Src family tyrosine kinase Hck. Nature **385:**602–609.
53. **Sigal, C. T., W. Zhou, C. A. Buser, S. McLaughlin, and M. D. Resh.** 1994. Amino-terminal basic residues of Src mediate membrane binding through electrostatic interaction with acidic phospholipids. Proc. Natl. Acad. Sci. U. S. A. **91:**12253–12257.
54. **Swaminathan, G., E. A. Feshchenko, and A. Y. Tsygankov.** 2007. c-Cbl-facilitated cytoskeletal effects in v-Abl-transformed fibroblasts are regulated by membrane association of c-Cbl. Oncogene **26:**4095–4105.
55. **Tanaka, T., J. B. Ames, T. S. Harvey, L. Stryer, and M. Ikura.** 1995. Sequestration of the membrane-targeting myristoyl group of recoverin in the calcium-free state. Nature **376:**444–447.
56. **Thomas, S. M., and J. S. Brugge.** 1997. Cellular functions regulated by Src family kinases. Annu. Rev. Cell Dev. Biol. **13:**513–609.
57. **van't Hof, W., and M. D. Resh.** 1999. Dual fatty acylation of p59(Fyn) is required for association with the T cell receptor zeta chain through phosphotyrosine-Src homology domain-2 interactions. J. Cell Biol. **145:**377–389.
58. **van't Hof, W., and M. D. Resh.** 1997. Rapid plasma membrane anchoring of newly synthesized p59fyn: selective requirement for NH2-terminal myristoylation and palmitoylation at cysteine-3. J. Cell Biol. **136:**1023–1035.
59. **Xu, W., A. Doshi, M. Lei, M. J. Eck, and S. C. Harrison.** 1999. Crystal structures of c-Src reveal features of its autoinhibitory mechanism. Mol. Cell **3:**629–638.
60. **Xu, W., S. C. Harrison, and M. J. Eck.** 1997. Three-dimensional structure of the tyrosine kinase c-Src. Nature **385:**595–602.
61. **Yokouchi, M., T. Kondo, A. Sanjay, A. Houghton, A. Yoshimura, S. Komiya, H. Zhang, and R. Baron.** 2001. Src-catalyzed phosphorylation of c-Cbl leads to the interdependent ubiquitination of both proteins. J. Biol. Chem. **276:**35185–35193.
62. **Zhang, J., F. J. Adrian, W. Jahnke, S. W. Cowan-Jacob, A. G. Li, R. E. Iacob, T. Sim, J. Powers, C. Dierks, F. Sun, G. R. Guo, Q. Ding, B. Okram, Y. Choi, A. Wojciechowski, X. Deng, G. Liu, G. Fendrich, A. Strauss, N. Vajpai, S. Grzesiek, T. Tuntland, Y. Liu, B. Bursulaya, M. Azam, P. W. Manley, J. R. Engen, G. Q. Daley, M. Warmuth, and N. S. Gray.** Targeting Bcr-Abl by combining allosteric with ATP-binding-site inhibitors. Nature **463:**501–506.